

Interactive Higher-order Network Analysis

Ryan A. Rossi
Adobe Research
rossi@adobe.com

Nesreen K. Ahmed
Intel Labs
nesreen.k.ahmed@intel.com

Eunye Koh
Adobe Research
eunye@adobe.com

Abstract—Higher-order network modeling and analysis is vital to understand the structures governing the configuration and behavior of complex networks. While network motifs are known to be fundamental building blocks of complex networks, the higher-order configuration and organization of complex networks remains widely unknown. In this work, we develop *interactive visual higher-order network mining and modeling techniques* to gain insight into the higher-order structure and composition of complex networks. The approach uncovers higher-order configurations including important phenotypes in a human gene interaction network and hubs in a power grid network.

Index Terms—Graph mining, higher-order network analysis, network motifs, graphlets, interactive visual graph mining

I. INTRODUCTION

Complex networks (graphs) arise ubiquitously in the natural world where entities (nodes) and their interactions (edges) are observed, *e.g.*, between humans [2], proteins [3], chemical compounds [4], neurons [5], [6], routers [7], web pages [8], devices & sensors [9], infrastructure (roads, airports, power stations) [1], economies [10], vehicles (cars, satellites, UAVs) [11], and information in general [12], [13]. Graphs (networks) also arise in a more unnatural and heuristic fashion by deriving a metric space between entities and retaining only the node pairs that are *significantly* “similar” [14].

Higher-order connectivity patterns are crucial to understand the structures governing the configuration and behavior of complex networks [15], [16]. The most common higher-order structures are small induced subgraphs referred to as network motifs (graphlets). More formally, a network motif (graphlet) $H_t = (V_k, E_k)$ is an induced subgraph consisting of a subset $V_k \subset V$ of k vertices from $G = (V, E)$ together with all edges whose endpoints are both in this subset $E_k = \{\forall e \in E \mid e = (u, v) \wedge u, v \in V_k\}$. Network motifs are building blocks of complex networks with applications in network alignment [17], classification [18], [19], dynamic network analysis [20], and link prediction [21]. The goal of *higher-order network analysis* is to gain new insights into the higher-order organization of complex networks.

In this work, we present a fast, flexible, and completely interactive visual network analytics platform that facilitates higher-order network modeling and analysis by allowing users to quickly uncover important higher-order structures as well as obtain insights into the higher-order organization of the network in real-time. To the best of our knowledge, this work is the first to define and investigate the problem of interactive visual higher-order network analysis that combines visual representations and interaction techniques with state-of-the-art

higher-order network analysis, modeling, and transformation methods. The goal of interactive higher-order network analysis is to enable users to quickly uncover important higher-order structures in networks to facilitate rapid situation assessment, planning, and decision making in real-time with minimum effort. Therefore, the platform is designed to be fast, easy-to-use, and intuitive allowing users to reveal the structure and higher-order organization of network data via intuitive visual representations and easy-to-use interaction techniques to explore higher-order network patterns in a free-flowing fashion in real-time (Figure 1).

This work enables users to interactively explore the higher-order structures and organization of networks in real-time by combining novel higher-order network modeling and analysis techniques with interactive visualizations. Previous work in interactive network visualization have used only rudimentary structural properties such as degree distribution and the ilk [22]–[27] and have not considered more advanced structural properties such as graphlet counts and other features derived from them.

II. APPROACH

The emergence and utility of graphlets (network motifs, induced subgraphs) in a variety of applications has given rise to many exact algorithms [19], [28]–[31] and estimation methods [32]–[36]. To derive the subgraph frequencies, we use fast parallel exact algorithms [15] or recent provably accurate estimation methods [32], [33]. The user has the ability to specify between either exact or estimation methods and if estimation is chosen the user can specify an error tolerance to ensure all estimates are within a guaranteed level of accuracy.

An overview of the platform is provided in Figure 1. We designed the *interactive higher-order network modeling and analysis platform* to be consistent with the way humans learn via *immediate-feedback* upon every user interaction [37]–[39]. For example, suppose the user begins lasso-selecting the nodes of interest by directly interacting with the node-link diagram, we immediately update all statistics, properties, models, and visual representations that require updating in real-time. Users have rapid, incremental, and reversible control over all visual graph queries with *immediate* and *continuous visual feedback* by strongly following the rules of direct manipulation [40] and dynamic (visual) querying [37], [41]. The web-based platform enables users to move from raw data to insights within seconds by simply dropping a graph file into the visualization window [39]. Despite the obvious advantages of a web-based

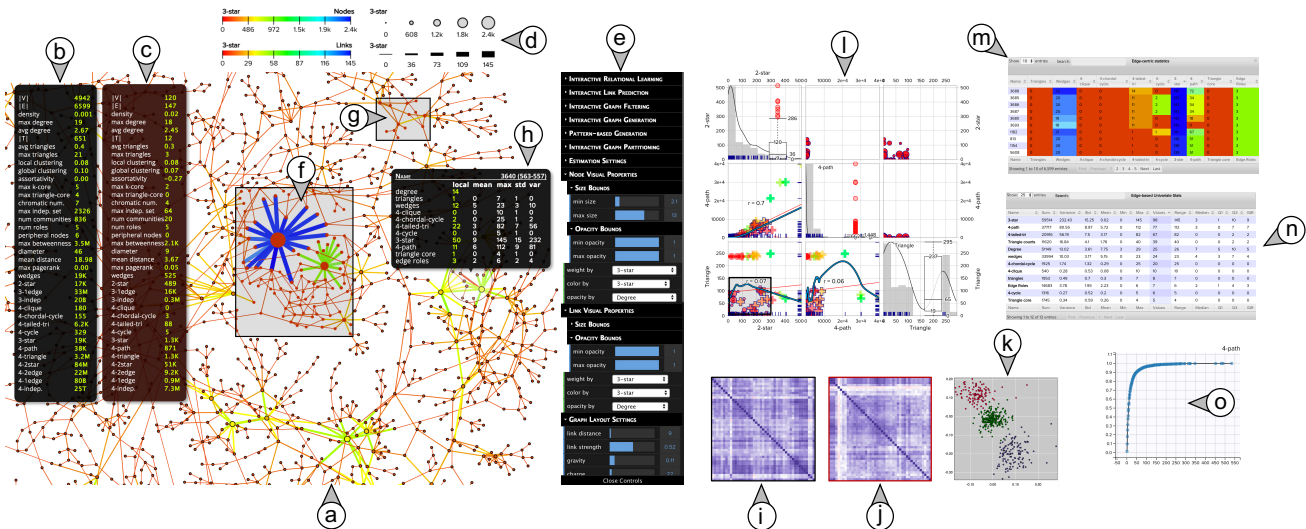


Fig. 1. Interactive higher-order network analysis of the US Power Grid network [1] consisting of substations (nodes) connected by high-voltage transmission lines (links). The main visualization window (a)-(h) includes (a) an interactive node-link diagram; (b) global higher-order network statistics of the entire graph and (c) the selected subgraph(s); (d) a legend summarizing the network motifs used to map the color, size, and opacity of nodes and edges; (e) an interactive interface for customizing and tuning interactive filters, visual properties of nodes and edges, etc; (f)-(g) interactive visual graph queries by lasso-selecting/brushing over a subgraph of interest by directly interacting with the node-link diagram; and (h) local higher-order network properties of a selected edge (or node). On the right of the main visualization window is (i) a linked interactive pairwise feature correlation matrix for the current set of higher-order features and (j) an interactive correlation matrix for the selected subgraph(s); (k) a two-dimensional higher-order embedding of the nodes; and (l) an interactive scatter plot matrix for exploring the local higher-order edge statistics; (m) interactive data table for local higher-order edge statistics and (n) global higher-order edge statistics (node data tables were removed for brevity); and (o) a cumulative distribution function (CDF) for a user-specified motif.

platform (e.g., it can be used directly in seconds, requires no installation, updates, etc.), previous work has mostly focused on offline platforms that must be downloaded and installed before using it [22], [24], [26].

The user can easily explore a variety of network motifs to gain insight into the higher-order organization by simply mapping the color, size, and opacity of nodes and edges to different network motifs and higher-order features derived by the user (Figure 1). Further, the user can generate new higher-order features from the current set using a variety of transformation functions, relational aggregations, and scaling functions. The higher-order features can also be used in interactive visual relational learning techniques for predictive modeling tasks such as node and link classification and prediction. To understand the relationships among the nodes (and edges), we embed the nodes into a K -dimensional space using network motifs [42] and then project back to two dimensional space for visualization; see Figure 1(k). All visualizations are interactive and support direct manipulation, brushing, linking, zooming, panning, tooltips, among others [43], [44]. To analyze the higher-order connectivity of nodes, links, and subgraphs (e.g., 4-clique motifs), one can simply select the ones of interest directly in the visualization window. Subgraphs may be directly selected by brushing over interesting regions of the network visually in the node-link diagram shown in Figure 1(a), scatter plot matrices shown in Figure 1(m), or one of the other interactive visual representations shown in Figure 1. Multiple selections from different regions of the graph are also supported and linked across the different interactive visual representations. Selected nodes,

links, and subgraphs may be removed, induced, or even moved by easily dragging them to the desired location. All global and local higher-order network properties are automatically updated in an efficient manner after each graph manipulation. Visualizations can be exported easily as high-quality images as well as (generated/transformed/filtered) graph data, attributes, learned models, among others. Visualizations can be exported easily as high-quality images as well as (generated/transformed/filtered) graph data, attributes, learned models, new features from various transformations, among other useful data derived through the visual analytic process. Graph file(s) can be quickly visualized and interactively explored in seconds by simply dropping them in the visualization window. A wide variety of graph formats are also supported including edge lists, adjacency lists, XML-based formats (gexf, graphml), and others (gml, json, net/pajek, mtx).

Interactive Motif-based Graph Exploration: Weighted motif graphs can often be used to uncover the important higher-order structures in a network. Given a network $G = (V, E)$ with $N = |V|$ nodes, $M = |E|$ edges, and a set $\mathcal{H} = \{H_1, \dots, H_T\}$ of T network motifs, we define \mathcal{W} as a motif tensor where $W_{ijt} =$ number of instances of motif (induced subgraph) $H_t \in \mathcal{H}$ that contain $(i, j) \in E$ and $W_{ijt} = 0$ if $(i, j) \notin E$ or if the motif $H_t \in \mathcal{H}$ does not co-occur between nodes i and j . For convenience, let \mathbf{W}_t denote the sparse weighted motif adjacency matrix for motif $H_t \in \mathcal{H}$. To generalize the above weighted motif graph formulation, we replace the edge constraint that ensures an edge exists between i and j if the number of instances of motif $H_t \in \mathcal{H}$ that contain nodes i and j is 1 or larger, with a constraint that requires each

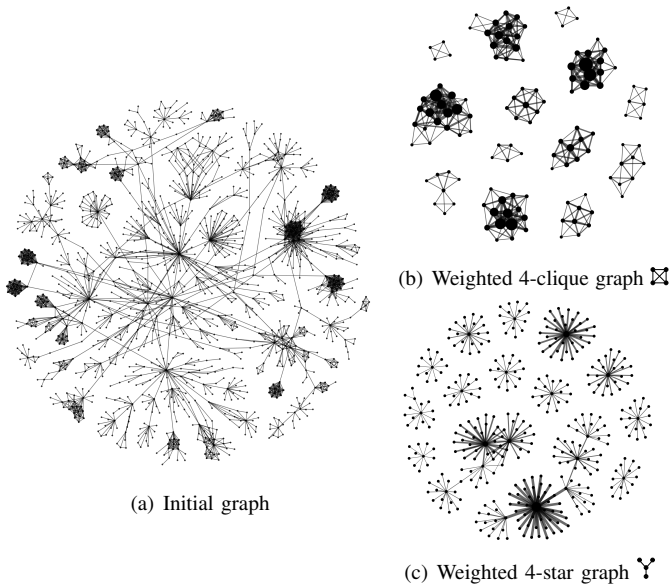


Fig. 2. **Interactive higher-order network analysis using the weighted motif graphs of interest (web-google).** Rich higher-order network structures are revealed immediately to the user in real-time upon selection of the motif graph of interest. Observe that as λ grows large, the number of disconnected components generally increases. Size (weight) of nodes and edges in the 4-clique \boxtimes and 4-star Υ motif graphs correspond to the frequency of 4-node cliques and 4-node paths, respectively.

edge to have at least λ motifs. Given an arbitrary weighted motif graph \mathbf{W} , we define $\mathbf{W}^{(\lambda)}$ for $\lambda > 0$ as:

$$\mathbf{W}_{ij}^{(\lambda)} = \begin{cases} W_{ij} & \text{if } W_{ij} \geq \lambda \\ 0 & \text{otherwise} \end{cases} \quad (1)$$

More generally, the user can define a constraint visually (*i.e.*, via a slider) as a type of range-based selection query that consists of two parameters including λ and Δ . One example of such a query is as follows: select all edges $(i, j) \in E$ such that $\lambda_t \leq W_{ijt} \leq \Delta_t$ for an arbitrary weighted motif graph \mathbf{W}_t . Such (λ, Δ) -weighted motif graphs are essentially the weighted motif graph resulting from a user-defined constraint encoded as a range-based selection query. The platform also allows the user to construct and visually explore new weighted graphs using one or more weighted motif graphs. For instance, $E_S = \{(i, j) \in E \mid (W_{ij1} \geq \lambda_1 \wedge W_{ij1} \leq \Delta_1) \wedge \dots \wedge (W_{ijt} \geq \lambda_t \wedge W_{ijt} \leq \Delta_t)\}$ where E_S is all the edges that satisfy the conjunctive motif-based query. However, we can also construct motif-based graphs using existential quantification that requires at least one of the user-defined constraints to be satisfied.

The above formulation allows the user to interactively explore new graphs that arise using the higher-order motif-based structures as a basis. The user can easily explore this space by adjusting a few simple sliders that control λ_t and Δ_t for each network motif of interest. As we have shown above, multiple interactive motif-based graph filters can also be visually configured by the user (*e.g.*, by adjusting a slider for each motif of interest). The visual representations are

updated immediately upon any change of the slider by the user. This makes it easy and intuitive for the user to visually explore and understand the impact of the user-defined motif-based range queries.

Motif graphs can be used to reveal the important higher-order structures (Figure 5). The motif graphs also facilitate navigation and exploration of large graphs. Visualizing large graphs using node-link diagrams suffer from visual clutter and computational issues that prohibit real-time visual graph mining and exploration. Many techniques have been proposed to navigate and explore large graphs using other types of visual representations [45]–[47]. Most of these approaches rely on other visual representations of the graph data such as a table of node attribute information, scatter plots, and clustering. However, motif graphs typically have a lot less nodes and edges (depending on the user-defined λ 's for the motif graph) and often gives rise to many interesting disconnected components that can be interactively explored (Figure 2). The interactive higher-order network analysis platform also provides techniques for interactive motif-based semi-supervised learning (SSL) [48]. These techniques can be used to explore the utility of motifs and higher-order features derived by the user for node and link classification.

III. RESULTS

The platform enables users to identify higher-order organization of complex networks in a completely visual and interactive fashion in real-time. Important hubs in the US power grid are identified by the approach (Figure 1). These

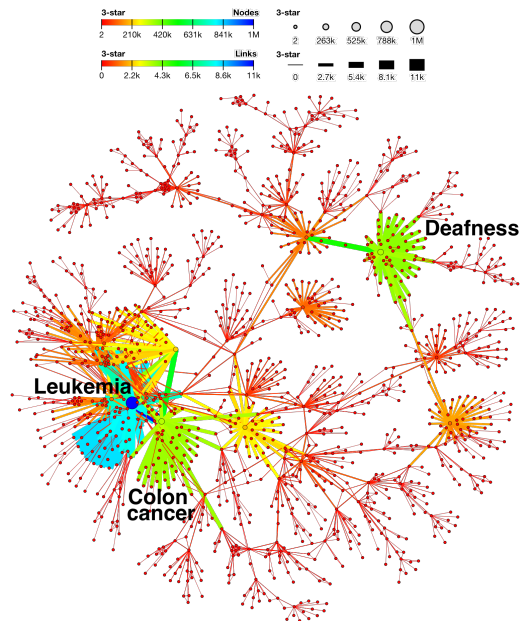


Fig. 3. **Higher-order analysis of a human gene disease interaction network** [49]. The interactive higher-order network analysis platform reveals the important phenotypes associated with diseases such as Leukemia, color cancer, and deafness (ordered by size). These phenotypes correspond to hubs (large stars) that connect to a number of distinct disorders which is consistent with [49].

appear as extrema when 4-node star motifs are used to capture hub-like structures in the US power grid. Results on a network of routers demonstrate how it reveals highly robust and fault tolerant systems of routers in the network topology (Figure 4). Other network motifs reveal potential congestion points and vulnerabilities in the router-level topology. The higher-order organizational structures identified from the approach can facilitate the design, planning, and vulnerability assessment of an organizations router-level topology. The topology of a network (connectivity of autonomous systems (ASes) or routers) has significant implications on the design of protocols and applications, and on the placement of services and data centers. Other applications of the interactive higher-order network analysis approach shown on the right in Figure 1 include detecting key transportation hubs in the international E-road network (Figure 6), identifying fundamental phenotypes in a human gene disease network, and finding important brain regions in the *C. elegans* neuronal network (Figure 7).

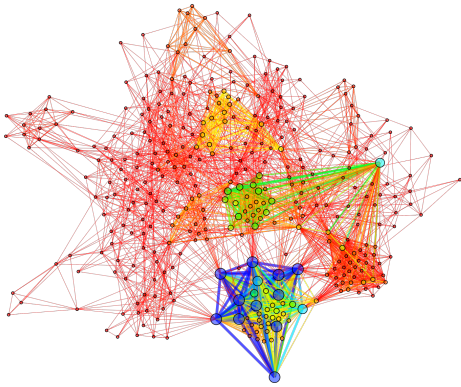


Fig. 4. **Higher-order analysis of a network of routers** [50]. The approach reveals highly robust and fault tolerant systems of routers. Routers & links are colored/weighted by 4-cliques.

Using the human gene disease network, we immediately uncover the important phenotypes such as leukemia, color cancer, and deafness (Figure 3). These phenotypes correspond to hubs (large stars) that connect to a number of distinct disorders which is consistent with [49].

In Figure 5, the four-star γ -graph immediately reveals the important higher-order structures. Using interactive filters, the user can explore combinations of the various motif graphs in real-time by adding any arbitrary combination of motif constraints, *e.g.*, show only the edges that are contained within at least one 4-star and 4-path. Hence, given a subgraph pattern of interest, the approach provides techniques for the user to interactively visualize and explore the space of potential motif graphs in real-time. In Figure 5, the researchers at the center of the three largest stars are Barabási, Newman, and Jeong (ordered by the size of the star). These researchers are hub-like in the sense that they connect many researchers whom would otherwise be disconnected. Obviously, removing these researchers would fracture the network into many disconnected components.

Fig. 3 and Fig. 5 demonstrate how the user can easily uncover the important higher-order structures and organization of the network by encoding the color and weight of nodes and links in the network using the counts of a few network motifs. In this way, we can leverage motifs to find and rank large stars, cliques, and other complex higher-order structures that are of fundamental importance in many types of networks [32].

Interactive higher-order graph mining also allows the user to quickly detect anomalies of interest in the graph. In Figure 2(b), we immediately obtain the large cliques in a web graph by deriving in real-time the λ -weighted 4-clique motif graph where λ is the cutoff such that if $W_{ij,t}$ is less than λ than it is removed. The edge set E_t for motif $H_t \in \mathcal{H}$ parameterized by λ is defined as $E_t = \{(i, j) \in E \mid W_{ij,t} \geq \lambda\}$ where $\lambda = 1$ in Figure 2(b)- 2(c). These large cliques observed in Figure 2(b) may pertain to link farms and collusion in the web hyperlink graph [52]. The large cliques are made up of many smaller 4-cliques (Figure 2(b)). In the platform, the user can explore the space of weighted motif graphs by simply using an interactive edge filter with the specific motif of interest. In Figure 2(b), this corresponds to simply using an interactive 4-clique filter to remove any edge with $W_{ij} < \lambda$ where $W_{ij} = \#$ of 4-cliques that contain $(i, j) \in E$. Using this interactive edge filter, the user can quickly understand the impact of different λ 's by simply adjusting a slider in real-time. This allows the user to explore in real-time the space of weighted motif graphs that arise from different choices of λ . Furthermore, this interactive exploration helps uncover the higher-order network organization and provides important insights into the motifs that are important for the particular

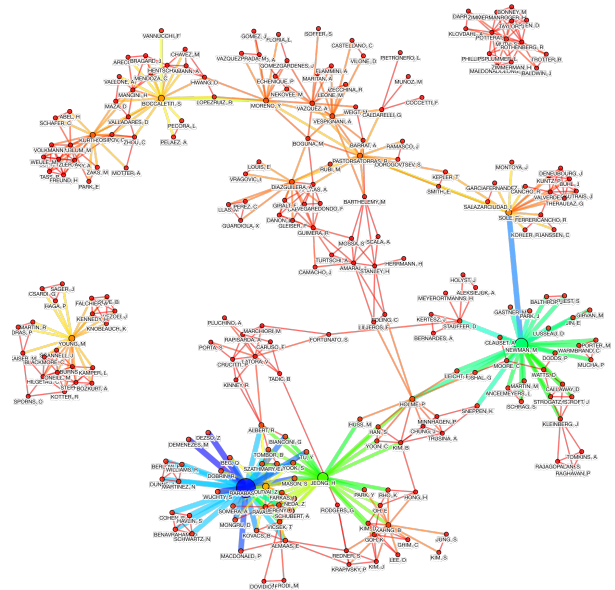


Fig. 5. **Interactively uncovering the higher-order network organization of a co-authorship graph (ca-netscience)** [2]. Nodes and links are colored and weighted by 4-stars. Important *higher-order structures* such as large stars and cliques can be uncovered in real-time and explored interactively by the user. Strikingly, the motif graphs clearly reveal the important higher-order structures. Large star subgraph patterns are immediately detected in the above figure and ranked from the largest star (blue) to smallest (red).

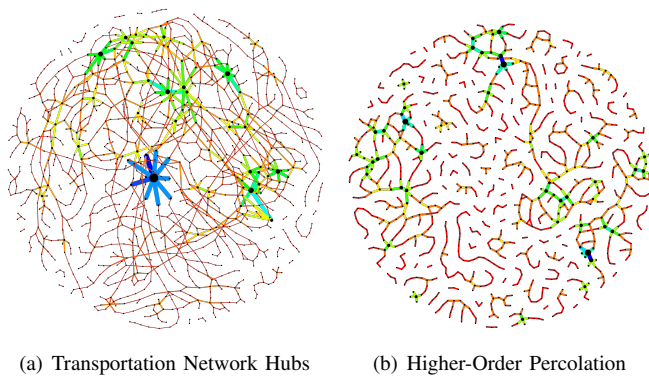


Fig. 6. **Higher-order network analysis of a European transportation network** [51]. Using the 4-node star motif the higher-order network analysis techniques reveal essential hubs in the European international road network. The impact on the network structure when these large hubs are removed is shown on the right. Using the higher-order structures identified by our approach in such investigations are important and useful for planning, simulations, and other important decision-making tasks.

network of interest. Although the original graph is connected (Figure 2(a)), the weighted motif graphs in Figure 2(b)-2(c) are shattered into many connected components that represent the largest cliques and stars in the network, respectively.

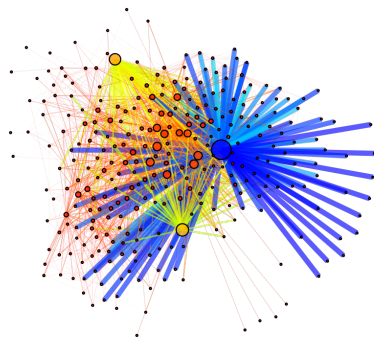


Fig. 7. **Higher-order network analysis of *c. elegans* neural activity.** Observe that the weighted 4-star motif graph immediately reveals the large stars in the graph as they are composed of many smaller 4-star motifs. In the above visualization, the links and nodes are colored and sized by the frequency of 4-star motifs.

Interactive higher-order network analysis is also useful for percolation studies [53]. By removing the largest hubs, the road network shatters into many disconnected components (Figure 6(b)). Depending on the structure of the network and the underlying process that governs the formation of the network, different motifs will be important for different graphs. Thus, interactive higher-order network analysis allows us to quickly understand the important motifs behind the structure of the network of interest as well as gain insights into the underlying process that governs the formation of the network that ultimately determines the motifs deemed important.

IV. CONCLUSION

We formulated interactive higher-order network analysis and introduced a visual network analytics platform for uncovering the higher-order configuration of complex networks. The platform allows the user to gain new insights into the higher-order configuration and organization of the network. Results indicate that complex networks contain non-trivial higher-order structural configurations that are quickly uncovered by the interactive visual analytic platform for higher-order network analysis. A video demo is also provided at:

<https://youtu.be/VE-GsP4p9n8>

REFERENCES

- [1] J.-W. Wang and L.-L. Rong, "Cascade-based attack vulnerability on the us power grid," *Safety Science*, vol. 47, no. 10, pp. 1332–1336, 2009.
- [2] M. E. Newman, "Finding community structure in networks using the eigenvectors of matrices," *Physical review E*, vol. 74, no. 3, p. 036104, 2006.
- [3] J. Kludas, M. Arvas, S. Castillo, T. Pakula, M. Oja, C. Brouard, J. Jäntti, M. Penttilä, and J. Rousu, "Machine learning of protein interactions in fungal secretory pathways," *PLoS one*, vol. 11, no. 7, p. e0159302, 2016.
- [4] V. Hatzimanikatis, C. Li, J. A. Ionita, C. S. Henry, M. D. Jankowski, and L. J. Broadbelt, "Exploring the diversity of complex metabolic networks," *Bioinformatics*, vol. 21, no. 8, pp. 1603–1609, 2005.
- [5] E. Bullmore and O. Sporns, "Complex brain networks: graph theoretical analysis of structural and functional systems," *Nature Rev. Neurosci.*, vol. 10, no. 3, pp. 186–198, 2009.
- [6] D. S. Bassett and E. Bullmore, "Small-world brain networks," *The neuroscientist*, vol. 12, no. 6, pp. 512–523, 2006.
- [7] R. A. Rossi, S. Fahmy, and N. Talukder, "A multi-level approach for evaluating internet topology generators," in *Networking*, 2013, pp. 1–9.
- [8] H. Ino, M. Kudo, and A. Nakamura, "Partitioning of web graphs by community topology," in *WWW*. ACM, 2005, pp. 661–669.
- [9] N. Eagle and A. S. Pentland, "Reality mining: sensing complex social systems," *Personal and ubiquitous computing*, vol. 10, no. 4, pp. 255–268, 2006.
- [10] F. Schweitzer, G. Fagiolo, D. Sornette, F. Vega-Redondo, A. Vespignani, and D. R. White, "Economic networks: The new challenges," *Science*, vol. 325, no. 5939, pp. 422–425, 2009.
- [11] S. Bhadra and A. Ferreira, "Complexity of connected components in evolving graphs and the computation of multicast trees in dynamic networks," in *ADHOC-NOW*, vol. 2865. Springer, 2003, pp. 259–270.
- [12] X. Yu, X. Ren, Y. Sun, Q. Gu, B. Sturt, U. Khandelwal, B. Norick, and J. Han, "Personalized entity recommendation: A heterogeneous information network approach," in *WSDM*, 2014, pp. 283–292.
- [13] R. A. Rossi and R. Zhou, "Parallel collective factorization for modeling large heterogeneous networks," *Social Network Analysis and Mining (SNAM)*, vol. 6, no. 1, p. 67, 2016.
- [14] X. Zhu, Z. Ghahramani, and J. D. Lafferty, "Semi-supervised learning using gaussian fields and harmonic functions," in *Proceedings of the 20th International conference on Machine learning (ICML-03)*, 2003, pp. 912–919.
- [15] N. K. Ahmed, J. Neville, R. A. Rossi, and N. Duffield, "Efficient graphlet counting for large networks," in *ICDM*, 2015, pp. 1–10.
- [16] A. R. Benson, D. F. Gleich, and J. Leskovec, "Higher-order organization of complex networks," *Science*, vol. 353, no. 6295, pp. 163–166, 2016.
- [17] M. Koyutürk, Y. Kim, U. Topkara, S. Subramaniam, W. Szpankowski, and A. Grama, "Pairwise alignment of protein interaction networks," *Journal of Computational Biology*, vol. 13, no. 2, pp. 182–199, 2006.
- [18] S. Vishwanathan, N. Schraudolph, R. Kondor, and K. Borgwardt, "Graph kernels," *JMLR*, vol. 11, pp. 1201–1242, 2010.
- [19] N. K. Ahmed, J. Neville, R. A. Rossi, N. Duffield, and T. L. Willke, "Graphlet decomposition: Framework, algorithms, and applications," *Knowledge and Information Systems (KAIS)*, pp. 1–32, 2016.
- [20] P. Basu, A. Bar-Noy, R. Ramanathan, and M. P. Johnson, "Modeling and analysis of time-varying graphs," *arXiv preprint arXiv:1012.0260*, 2010.
- [21] M. Rahman and M. Al Hasan, "Link prediction in dynamic networks using graphlet," in *ECML PKDD*, 2016, pp. 394–409.

- [22] D. Auber, "Tulip – a huge graph visualization framework," in *Graph Drawing Soft.*, 2004, pp. 105–126.
- [23] B.-J. Breitkreutz, C. Stark, and M. Tyers, "Osprey: a network visualization system," *Gen. bio.*, vol. 4, no. 3, 2003.
- [24] M. Bastian, S. Heymann, M. Jacomy *et al.*, "Gephi: an open source software for exploring and manipulating networks." *ICWSM*, vol. 8, pp. 361–362, 2009.
- [25] M. E. Smoot, K. Ono, J. Ruschinski, P.-L. Wang, and T. Ideker, "Cytoscape 2.8: new features for data integration and network visualization," *Bioinformatics*, vol. 27, no. 3, pp. 431–432, 2010.
- [26] M. Xia, J. Wang, and Y. He, "Brainnet viewer: a network visualization tool for human brain connectomics," *PLoS one*, vol. 8, no. 7, p. e68910, 2013.
- [27] V. Batagelj and A. Mrvar, "Pajek – analysis and visualization of large networks," in *Graph drawing software*. Springer, 2004, pp. 77–103.
- [28] S. Wernicke and F. Rasche, "Fanmod: a tool for fast network motif detection," *Bioinformatics*, vol. 22, no. 9, pp. 1152–1153, 2006.
- [29] D. Marcus and Y. Shavitt, "Rage—a rapid graphlet enumerator for large networks," *Computer Networks*, vol. 56, no. 2, pp. 810–819, 2012.
- [30] T. Hočevar and J. Demšar, "A combinatorial approach to graphlet counting," *Bioinformatics*, vol. 30, no. 4, pp. 559–565, 2014.
- [31] T. Milenković, J. Lai, and N. Pržulj, "Graphcrunch: a tool for large network analyses," *BMC bioinformatics*, vol. 9, no. 1, p. 1, 2008.
- [32] N. K. Ahmed, T. L. Willke, and R. A. Rossi, "Estimation of local subgraph counts," in *BigData*, 2016, pp. 1–10.
- [33] R. A. Rossi, R. Zhou, and N. K. Ahmed, "Estimation of graphlet counts in massive networks," in *IEEE Transactions on Neural Networks and Learning Systems (TNNLS)*, 2018, pp. 1–14.
- [34] M. Jha, C. Seshadhri, and A. Pinar, "Path sampling: A fast and provable method for estimating 4-vertex subgraph counts," in *WWW*, 2015.
- [35] M. Rahman, M. A. Bhuiyan, M. Rahman, and M. Al Hasan, "GUISE: A uniform sampler for constructing frequency histogram of graphlets," *KAIS*, vol. 38, no. 3, pp. 511–536, 2014.
- [36] M. Rahman, M. Bhuiyan, M. Al Hasan *et al.*, "GRAFT: An efficient graphlet counting method for large graph analysis," *TKDE*, vol. 26, no. 10, pp. 2466–2478, 2014.
- [37] C. Ahlberg, C. Williamson, and B. Shneiderman, "Dynamic queries for information exploration: An implementation and evaluation," in *Proc. of SIGCHI*, 1992, pp. 619–626.
- [38] J. J. Thomas and K. A. Cook, *Illuminating the Path: the research and development agenda for visual analytics*. IEEE Computer Society, 2005.
- [39] N. K. Ahmed and R. A. Rossi, "Interactive visual graph analytics on the web," in *ICWSM*, 2015, pp. 566–569.
- [40] B. Shneiderman, "Direct manipulation for comprehensible, predictable and controllable user interfaces," in *IUI*. ACM, 1997, pp. 33–39.
- [41] ———, "Dynamic queries for visual information seeking," *IEEE software*, vol. 11, no. 6, pp. 70–77, 1994.
- [42] R. A. Rossi, N. K. Ahmed, and E. Koh, "Higher-order network representation learning," in *Proceedings of the 23rd International Conference Companion on World Wide Web (WWW)*, 2018.
- [43] J. S. Yi, Y. ah Kang, and J. Stasko, "Toward a deeper understanding of the role of interaction in information visualization," *TVCG*, vol. 13, no. 6, pp. 1224–1231, 2007.
- [44] M. Q. Wang Baldonado, A. Woodruff, and A. Kuchinsky, "Guidelines for using multiple views in information visualization," in *AVI*, 2000.
- [45] A. Bezerianos, F. Chevalier, P. Dragicevic, N. Elmqvist, and J.-D. Fekete, "Graphdice: A system for exploring multivariate social networks," in *Computer Graphics Forum*, vol. 29, no. 3. Wiley Online Library, 2010, pp. 863–872.
- [46] N. Elmqvist, T.-N. Do, H. Goodell, N. Henry, and J.-D. Fekete, "Zame: Interactive large-scale graph visualization," in *PacificVIS*, 2008, pp. 215–222.
- [47] Y. Hu and L. Shi, "Visualizing large graphs," *Wiley Interdisciplinary Reviews: Comp. Stat.*, vol. 7, no. 2, pp. 115–136, 2015.
- [48] R. A. Rossi, R. Zhou, and N. K. Ahmed, "Relational similarity machines," in *MLG*, 2016, p. 8.
- [49] K.-I. Goh, M. E. Cusick, D. Valle, B. Childs, M. Vidal, and A.-L. Barabási, "The human disease network," *PNAS*, vol. 104, no. 21, pp. 8685–8690, 2007.
- [50] N. Spring, R. Mahajan, and D. Wetherall, "Measuring isp topologies with rocketfuel," *SIGCOMM Computer Communication Review*, vol. 32, no. 4, pp. 133–145, 2002.
- [51] L. Šubelj and M. Bajec, "Robust network community detection using balanced propagation," *Eur. Phys. J. B*, vol. 81, no. 3, pp. 353–362, 2011.
- [52] L. Becchetti, C. Castillo, D. Donato, S. Leonardi, and R. A. Baeza-Yates, "Link-based characterization and detection of web spam," in *AIRWeb*, 2006, pp. 1–8.
- [53] C. Moore and M. Newman, "Epidemics and percolation in small-world networks," *Physical Review E*, vol. 61, no. 5, pp. 5678–5682, 2000.